HHS Public Access

Author manuscript

Abdom Radiol (NY). Author manuscript; available in PMC 2022 June 01.

Published in final edited form as:

Abdom Radiol (NY). 2021 June ; 46(6): 2556–2566. doi:10.1007/s00261-020-02892-x.

Added value of deep learning-based liver parenchymal CT volumetry for predicting major arterial injury after blunt hepatic trauma: a decision tree analysis

David Dreizin, MD* **[Associate Professor]**,
Emergency and Trauma Imaging, Department of Diagnostic Radiology and Nuclear Medicine, R Adams Cowley Shock Trauma Center, University of Maryland School of Medicine, Baltimore, MD

Tina Chen, BS,
Department of Diagnostic Radiology and Nuclear Medicine, University of Maryland School of Medicine, Baltimore, MD

Yuanyuan Liang, PhD [Professor],
Department of Epidemiology and Public Health, University of Maryland School of Medicine, Baltimore, MD

Yuyin Zhou,
Department of Computer Science, Center for Cognition Vision and Learning, Johns Hopkins University, Baltimore, MD

Fabio Paes, MD, MBA [Assistant Professor of Radiology],
Emergency and Trauma Imaging, Department of Radiology, University of Miami - Miller School of Medicine, Jackson Memorial Hospital - Ryder Trauma Center

Yan Wang, PhD,
Department of Computer Science, Center for Cognition Vision and Learning, Johns Hopkins University, Baltimore, MD

Alan L. Yuille, PhD [Bloomberg Distinguished Professor],
Department of Computer Science, Head, Center for Cognition Vision and Learning, Johns Hopkins University, Baltimore, MD

Patrick Roth, MD,
Emergency and Trauma Imaging, Department of Radiology, University of Miami - Miller School of Medicine, Jackson Memorial Hospital - Ryder Trauma Center

Kathryn Champ, MSIII,

*Corresponding Author: David Dreizin, MD, University of Maryland School of Medicine, 655 W Baltimore St., Baltimore, MD 21201, 410-238-5803, daviddreizin@gmail.com.

Conflict of interest: David Dreizin is founder of TraumaVisual, LLC

List of meetings at which the work was presented: none.

Department of Diagnostic Radiology and Nuclear Medicine, University of Maryland School of Medicine, Baltimore, MD

Guang Li, PhD [Assistant Professor],
Department of Diagnostic Radiology and Nuclear Medicine, University of Maryland School of Medicine, Baltimore, MD

Ashley McLenithan, BS,
R Adams Cowley Shock Trauma Center, University of Maryland School of Medicine, Baltimore, MD

Jonathan J. Morrison, MD, PhD [Assistant Professor]
Vascular Surgery, R Adams Cowley Shock Trauma Center, University of Maryland School of Medicine, Baltimore, MD

Abstract

Purpose: In patients presenting with blunt hepatic injury (BHI), the utility of CT for triage to hepatic angiography remains uncertain since simple binary assessment of contrast extravasation (CE) as being present or absent has only modest accuracy for major arterial injury on digital subtraction angiography (DSA). American Association for the Surgery of Trauma (AAST) liver injury grading is coarse and subjective, with limited diagnostic utility in this setting. Volumetric measurements of hepatic injury burden could improve prediction. We hypothesized that in a cohort of patients that underwent catheter directed hepatic angiography following admission trauma CT, a deep learning quantitative visualization method that calculates % liver parenchymal disruption (the LPD index, or LPDI) would add value to CE assessment for prediction of major hepatic arterial injury (MHAI).

Methods: This retrospective study included adult patients with BHI between 1/1/2008–5/1/2017 from two institutions that underwent admission trauma CT prior to hepatic angiography (n=73). Presence (n=41) or absence (n=32) of MHAI (pseudoaneurysm, AVF, or active contrast extravasation on DSA) served as the outcome. Voxelwise measurements of liver laceration were derived using an existing multiscale deep learning algorithm trained on manually labeled data using cross-validation with a 75–25% split in four unseen folds. Liver volume was derived using a pre-trained whole liver segmentation algorithm. LPDI was automatically calculated for each patient by determining the percentage of liver involved by laceration. Classification and regression tree (CART) analyses were performed using a combination of automated LPDI measurements and either manually segmented CE volumes, or CE as a binary sign. Performance metrics for the decision rules were compared for significant differences with binary CE alone (the current standard of care for predicting MHAI), and the AAST grade.

Results: 36% of patients (n = 26) had contrast extravasation on CT. Median [Q1-Q3] automated LPDI was 4.0% [1.0–12.1%]. 41/73 (56%) of patients had MHAI. A decision tree based on auto-LPDI and volumetric CE measurements (CEvol) had the highest accuracy (0.84, 95% CI: 0.73–0.91) with significant improvement over binary CE assessment (0.68, 95% CI: 0.57–0.79; p = 0.01). AAST grades at different cut-offs performed poorly for predicting MHAI, with accuracies ranging from 0.44–0.63. Decision tree analysis suggests an auto-LPDI cut-off of ≥ 12% for minimizing false negative CT exams when CE is absent or diminutive.

Conclusion: Current CT-imaging paradigms are coarse, subjective, and limited for predicting which BHIs are most likely to benefit from AE. LPDI, automated using deep learning methods, may improve objective personalized triage of BHI patients to angiography at the point of care.

Keywords

Blunt Hepatic Injury (BSI); Computed tomography (CT); Liver parenchymal disruption index (LPDI) Deep Learning (DL); Quantitative Imaging

Introduction

Blunt hepatic injuries (BHIs) are identified in up to one quarter of patients admitted with severe blunt trauma who undergo whole-body computed tomography (CT) (1). In those patients who are sufficiently stable to undergo admission CT, the presence of hepatic arterial contrast extravasation (CE) predicts future deterioration from arterial injury that is potentially reversible with angioembolization (AE) (2). Both CT and digital subtraction angiography (DSA) have contributed to a substantial increase in the proportion of patients with hepatic injuries who can be treated successfully with non-operative management (NOM) (3). CT is also used to predict which patients with high grade liver injury will have vascular lesions on angiography that would benefit from perioperative AE (4). However, published accuracies of CT in the triage of patients with BHI to angiography have been modest. CT contrast extravasation is the most direct sign of arterial bleeding but can be discordant with findings on angiography. In 2011, Letoublon *et al.* reported that 21% of patients with hepatic angiography performed for CE on CT did not require AE (5). Other authors have reported modest sensitivity (63–83%) and specificity (67–75%), and weak positive likelihood ratios (1.9–3.3) for binary CE evaluation (i.e. assessment as either positive or negative) on pre- and perioperative contrast-enhanced CT (CECT) in predicting the need for urgent hemostatic intervention (4, 6).

The current standard of care involves approaching CE on CT imaging as a binary univariate predictor (4, 6). Emphasis has been placed on the importance of CE because high-grade injuries may respond favorably to conservative treatment when CE is absent (7). But, the absence of CE on computed tomography does not entirely exclude significant hepatic arterial injury from declaring itself angiographically in patients with high American Association for the Surgery of Trauma (AAST) liver injury grade (4–6). If the absence of CE does not confidently exclude major hepatic arterial injury (MHAI), the validity of using this imaging sign to determine appropriate management in patients with high AAST grade injuries is uncertain. The AAST liver injury scale has traditionally served a complementary role in determining angiopositivity on catheter angiography and need for AE in patients without CE on CT scan and is heavily based on size and extent of liver laceration and hematoma. However this is a coarse categorical system that relies primarily on subjective assessment of the depth of parenchymal disruption and number of Couinaud segments involved (8).

Angiography is resource intensive with a small but non-negligible bleeding risk inherent to any invasive vascular procedure. Furthermore, biliary complications from hepatic necrosis

are relatively uncommon but increase in incidence with high grade injury (3, 9, 10) and may be exacerbated when AE is performed (11, 12).

Further improvement in the diagnostic utility of CT as a triage tool in patients with BHI could be achieved by leveraging voxelwise quantitative information (i.e. CT volumetry) to measure the degree of parenchymal injury and combine this data with CE assessment for more objective and explanatory personalized prediction. In this work, we re-trained and validated previously described deep learning (DL) algorithms for the task of automated measurement of the liver parenchymal disruption index (auto-LPDI), which we defined as the volume of laceration and intervening hematoma normalized to total hepatic volume on admission contrast-enhanced CT.

We hypothesized that this automated quantitative visualization tool could provide added value as an independent predictor of major hepatic arterial injury (MHAI) in a cohort of BHI patients that underwent catheter angiography following admission CT. The potential diagnostic value of volumetric CE measurements (CEvol), which currently require manual segmentation, was also assessed. Performance was interrogated using decision tree analysis. Multivariable analysis with logistic regression was used to determine the strength and significance of LPDI as an independent predictor.

Methods

Dataset and inclusion criteria

This HIPAA compliant and IRB approved retrospective study included 73 consecutive adult patients (age ≥ 18 years) between January 1, 2008 to May 1, 2017 with BHI who underwent contrast enhanced admission CT of the abdomen followed by hepatic arterial angiography at one of two level I trauma centers (56 patients from University of Maryland/R. Adams Cowley Shock Trauma Center, and 17 patients from University of Miami/Ryder Trauma Center). Patients who underwent angiography or laparotomy before CT were excluded. A positive outcome (MHAI) was defined as pseudoaneurysm, AVF, or active contrast extravasation on catheter-directed angiography.

Voxelwise ground truth labeling of CT scans

At both institutions, admission CT images were acquired on trauma bay-adjacent scanners in all patients through the entire torso in the arterial phase and through the upper abdomen in the portal venous phase and archived at 3 mm section thickness throughout the study period. At the R Adams Cowley Shock Trauma Center (STC), a 40-section and 64-section scanner (Brilliance; Philips Healthcare, Andover, Mass) were used from the start of the study period until July 2016, when the 40-section scanner was replaced with a dual source 128-section scanner (Somatom Force; Siemens Healthcare, Malvern, PA). At the Ryder Trauma Center (RTC), the same two 64-section CT scanners (Somatom Definition; Siemens Healthcare) were used throughout the study period. At both trauma centers, portal venous phase (PVP) images of the upper abdomen were routinely acquired from the dome of the diaphragm to the iliac crest. At STC, bolus tracking was used in the descending aorta with a 120 HU trigger for the initial arterial scan, and a delay range of ~60–70s for PVP images. At RTC, a

fixed delay of 70 seconds is employed. Settings across scanners and institutions included: 120 kVp, 250 mAs, 0.7 pitch, 0.5 second rotation time, and 0.625 collimation. Studies were archived at 3 mm section thickness at both centers.

For the purposes of imaging labeling and algorithm training, images were converted from Digital Imaging and Communications in Medicine (DICOM) into Neuroimaging Informatics Technology Initiative (NifTI) format. Bilinear interpolation was used to resample 512 × 512 matrix axial images to a 1.5 mm section thickness prior to reconstruction in sagittal and coronal planes.

Portal venous phase images (which confer peak hepatic parenchymal enhancement and optimal visualization of parenchymal disruption) were used for all labeling and volumetric measurements including a) total LPD volume, b) total liver volume, c) subcapsular hematoma volume, and d) CE volume. All voxelwise labeling was performed by research staff under the supervision of a radiologist with trauma subspecialization who reviewed the labels for quality and performed editing for all cases. Manual labeling and volumetric analysis were performed using an open-source software platform with an adjustable spherical threshold paint tool at Hounsfield Unit (HU) ranges set to approximately 10–80 HU (3D slicer, version 4.10, slicer.org) for laceration and subcapsular hematoma, 10–130 HU for whole liver, and ≥150 HU for CE. Labeling was performed in the axial plane although this is an inherently 3D method given the use of a spherical brush tool. In all studies, further supervision and editing was performed in the sagittal and coronal planes. Morphological smoothing filters were uniformly applied to reduce label artifact related to image noise (13). Using a range of HU values for annotation of each feature, quality control by an experienced trauma radiologist, editing in three planes, and the use of smoothing filters ensured labeling uniformity despite some differences in scanner makes, models, and protocols across institutions.

Deep learning algorithms: Implementation for quantitative visualization of LPDI

To derive automated LPDIs, we employed an existing pre-trained deep learning algorithm for automated liver whole-organ segmentation (14), and a recently-published deep learning algorithm robust for segmentation of pathology with widely variable sizes, shapes, and number of lesion foci previously used for multifocal active bleed segmentation (15) and quantitative visualization of hemoperitoneum (16), implemented here for liver parenchymal disruption. Specific technical details regarding architecture, training details, and implementation, are found in the following recently published works (15, 16). The algorithm uses a combination of attentional networks and dilated convolutional neural networks (CNNs) which are ideal for learning feature representations at multiple scales of a given image (15, 17). This can be thought of as similar to viewing pathologic specimens at different levels of magnification; fine detail is captured at small scales and detection of multiple lesions of varying sizes at progressively larger scales. Using transfer learning, all model weights were carried over from a prior implementation (in this case, for pelvic active bleeding) (18), and iteratively updated until the algorithm was optimally trained for the novel segmentation task (i.e. liver parenchymal disruption) (19). Training of the latter algorithm was performed in four folds, each consisting of a different combination of 3/4ths

of the total dataset. Testing was performed on the remaining unseen 1/4 of the data in each of the four-folds, resulting in automated labels in each patient. The automated labels for whole-liver and laceration segmentation are visualized as contours in a slice-by-slice scroll-through of the CT image (see Fig 1). Volumes are quantified by automated counting of the number of segmented voxels. A final step involves automatically calculating LPDI as the ratio of laceration volume to whole liver volume (both in mL).

Clinical data extraction

Relevant baseline characteristics, clinical and laboratory values, hepatic AAST grade, and the following outcomes were collected from the trauma registry and electronic medical record: 1. presence or absence of a major arterial vascular lesion at angiography (pseudoaneurysm, CE, or AVF), 2. whether hepatic AE was performed for the arterial lesion, and 3. whether angiography was performed perioperatively as an adjunct to hepatorrhaphy. If AE was performed strictly for prophylaxis (n = 3) the outcome was considered negative for the purposes of this study. If arterial bleeding was explicitly described in the operative report, treated intraoperatively, and followed by an angiogram that demonstrated resolution, the outcome was considered positive for MHAI (n = 2).

Data analysis: summary statistics

Summary statistics for baseline clinical and demographic characteristics, CEvol, auto-LPDI, and subcapsular hematoma volume were determined for the study population and compared across subsets of patients who did and did not have MHAI. All continuous variables were tested for normality using the Shapiro Wilk test. Student's t-test was used to compare means for normally distributed variables and the Mann-Whitney U test was used to compare medians for non-normally distributed variables. Fisher exact test was used to compare the association between two categorical variables.

Data analysis: Deep learning method evaluation

Deep learning method evaluation was performed using the following tests- Pearson's r and intraclass correlation coefficient (ICC) were used to assess correlation and agreement between manual and automated measurements for liver laceration, whole liver volume, and LPDI. Pearson's $r \geq 0.80$ and ICC ≥ 0.75 are considered strong correlation and excellent agreement respectively (20, 21). The Dice similarity coefficient (DSC), a measure of spatial overlap, was used to compare manual and automated whole liver and laceration labels; Bland-Altman plots were generated for the final output (LPDI) to determine 95% limits of agreement and measurement bias between methods.

Data analysis: diagnostic performance

Decision tree analyses were performed using the following two sets of parameters: 1. LPDI with binary CE, and 2. LPDI with CEvol. We employed the classification and regression tree (CART) approach (22) to generate decision rules for discrete or continuous biomarkers including optimal cut-offs for the latter. Diagnostic performance of the decision rules was compared with binary CE assessment using McNemar's tests for accuracy, sensitivity and specificity, and Z tests for predictive values (23). Logistic regression models including LPDI

and either CEvol or binary CE were used to determine whether LPDI was independently predictive of MHAI. The same accuracy metrics were also determined for the AAST hepatic organ injury scale at different cut-offs as a baseline comparison. One patient did not have a prospectively assigned liver AAST grade and was excluded from relevant comparisons. In all cases, p-values < 0.05 were considered statistically significant. Stata/SE version 16 (Stata, College Station, TX) and R Version 4.0.0 (R Core Team, 2020 and R Foundation for Statistical Computing, Vienna, Austria; https://www.R-project.org) was used for all statistical analyses.

Results

Patient characteristics

The study population consisted of 73 patients presenting with liver trauma from blunt injury mechanisms who underwent angiography following admission CT. At both institutions, triage to angiography is heuristic and dependent on institutional preferences and individual surgeon or angiographer judgement.

Summary statistics of baseline characteristics and timing of exams are presented for the total study population, and by individual institution in Table 1. Subsets of patients with and without MHAI are also presented. A comparison of volumetric and categorical imaging features is presented in Table 2. Visual results of automated LPDI in an example test case are shown in Figure 1. Fifty-five percent of patients were male (n = 40), and 45% were female (n = 33). Mechanism of injury was motor vehicle collision in 77% of patients, fall in 7%, and other mechanisms in the remaining 16%. Median [Q1, Q3] injury severity score (ISS) was 34 [27, 41]. Fifty-nine patients (81% of the cohort) underwent angiography as part of NOM. Angiography was performed as an adjunct to laparotomy in 14 patients (19% of the cohort). Seven patients (10%) were hypotensive despite triage to the CT scanner prior to intervention, and 43 patients (59%) had tachycardia. Four patients expired during hospitalization, three from non-survivable (AIS grade 6) head injuries and 1 patient from multiorgan system failure. Splenic injuries were the most common associated injuries seen in 43% of patients. 92% of patients had AAST Grade 3 or higher liver injuries (n = 66). Forty-one patients (56%) had major hepatic arterial injury while 32 (44%) did not.

Of the 41 patients with MHAI, 38 patients had angiographically proven active extravasation (n = 27), AVF (n = 6), and pseudoaneurysm (n = 4). AE was performed in all but one of these patients for whom there was a perceived risk of non-target embolization. Three patients had arterial bleeding diagnosed and managed operatively. A comparison of patients who did and did not undergo AE showed no significant differences in baseline characteristics including patient demographics, ISS, or vital signs.

Patients with MHAI had a higher proportion of CE on admission CT scan than patients without MHAI ($p < 0.001$). Differences in AAST liver injury grades did not reach statistical significance ($p = 0.08$), however auto-LPDI was significantly higher in the MHAI group ($p < 0.001$). Manual CEvol measurements were also higher ($p < 0.001$). A measurable subcapsular hematoma was present in only three patients. The parameter was not included in

decision tree analysis or model building due to the small patient number. A low prevalence of subcapsular hematoma has been reported previously by other authors (1).

Automated LPDI method evaluation

Automated volumetric results from four-fold cross-validation showed excellent correlation and agreement between manual and automated measurements for laceration volume (ICC = 90; r = 0.93), whole liver volume (ICC = 0.98; r = 0.98), and LPDI (ICC = 0.90; r = 0.94). DSC for whole liver volume was 0.95 (+/− SD 0.09), and for laceration volume was 0.65 (+/− SD 0.24). DSC is highly dependent on the relative size of the target in a fixed-size region of interest, and values in this range are common for variably-sized irregular targets (24). A bland-Altman plot showed a small systematic undermeasurement of LPDI of 2.2%, with limits of agreement of two standard deviations between −5.5–9.8%. The high degree of correlation, agreement for volumetric measurements, low bias of the LPDI, and the explainability of visual results (see Fig 1) all support the internal validity of the method.

Diagnostic performance

Binary CE, decision tree, and AAST diagnostic performance is summarized in Table 3. Hepatic AAST grade had poor accuracies at all thresholds ranging from 0.44–0.63. Cut-offs of grades 4 and 5 had poor positive and negative predictive value for MHAI. Accuracy of binary CE was 0.68 (0.57–0.79).

Logistic regression showed that both binary CE (p = 0.022; odds ratio (95% CI) = 4.55 (1.24–16.70)) and auto-LPDI (p = 0.014; unit-odds ratio (95% CI) = 1.12 (1.02–1.23)) are significant and independent predictors of MHAI. Decision tree analysis combining binary CE with auto-LPDI (decision rule 1) increased accuracy (95% CI) to 0.77 (0.65–0.86) with p-value approaching significance (p = 0.11) compared with binary CE. Further improvement over binary CE assessment was achieved for decision tree analysis combining CEvol and auto-LPDI (decision rule 2) with accuracy of 0.84 (95% CI: 0.73–0.91, p = 0.01).

Decision rule 1 resulted in seven fewer false negative CT exams (a 32% reduction) than binary CE assessment, with no change in false positives. Decision rule 2 resulted in twelve fewer false negative CT exams (a 63% reduction) with one additional false positive CT, increasing from 4 to 5 (25% change) (Figure 2 and Table 3).

High PPVs were maintained across the board for binary CE, decision rule 1, and decision rule 2 (84.6%, 87.5%, and 87.2% respectively), but sensitivities and NPVs increased substantially over binary CE assessment for decision rule 2 (sensitivity: 82.9% versus 53.7%, p-value<0.001; NPV: 79.4% versus 59.6%, p-value=0.06).

Discussion

CT combined with selective catheter angiography have both contributed to the widespread adoption of NOM in stable patients with BHIs (1–3, 7, 9). There has also been a trend across level I trauma centers toward more liberal utilization of CT as an initial tool for triage and treatment planning in more severely injured patients, including transient responders and patients with shock (25). In such patients, catheter angiography is also performed for

suspected MHAI as an adjunct to laparotomy (4, 26). In our study cohort, 10% of BHI patients that went on to catheter angiography following admission CT were hypotensive, and in 19%, angiography was undertaken perioperatively. Triage of BHI patients to angiography is largely based on a) presence or absence of CE on the initial scan, and b) assessment of liver parenchymal disruption using the AAST liver injury scale. However, accuracy of CT for MHAI remains modest (4–6, 27).

Granular voxelwise CT assessment of liver injury severity could be complementary for resolving ambiguous cases, particularly in those patients with high-grade liver injury for whom CE foci are absent or diminutive in size. However, the AAST liver injury grade is a coarse categorical framework that incorporates subjective semi-quantitative assessment of the degree of liver parenchymal disruption, and may be ill-suited for this purpose (8). For example, grade IV lacerations bin a wide spectrum of parenchymal disruption (25–75% of a hepatic lobe or 1–3 Couinaud segments) into a single tranche. The ambiguity could potentially result in delayed triage to the angiography suite in some patients, or non-therapeutic catheter-directed angiography in others. While most clinical and laboratory information is inherently quantitative and granular, CT interpretation leaves considerable unused volumetric quantitative information on the reading room or CT console table (28–30). There is inherent information loss that could be avoided with voxel-level volumetric measurements. To this end, we re-trained existing deep learning (DL) algorithms for quantitative visualization of the liver parenchymal disruption index (auto-LPDI).

We hypothesized that the accuracy of CT for predicting MHAI could be significantly higher than binary CE assessment using classification and regression tree analyses that incorporate auto-LPDI. Two decision rules were generated and tested against binary CE assessment. Decision rule 1 combined auto-LPDI with binary CE assessment, and decision rule 2 combined auto-LPDI with voxelwise CE volume (CEvol). We also used logistic regression to determine whether auto-LPDI was independent of CE in predicting MHAI.

We found that binary CE and auto-LPDI were independent predictors of MHAI. The unit-odds ratio of 1.12 for auto-LPDI indicates that for each 1% change in auto-LPDI, there is a corresponding 12% increase in the odds of MHAI. The accuracy of decision rule 1 (0.77) was improved over binary CE assessment alone (0.68), with a p-value that approached significance ($p = 0.11$). The accuracy of decision rule 2 which utilized CEvol and auto-LPDI resulted in an accuracy of 0.84, which was significantly improved over binary CE assessment (0.68, $p = 0.01$). In comparison, the accuracy of the AAST liver injury scale at thresholds of grade II-V ranged from only 0.44–0.63.

Decision rule 1 dictates that if there is a small (< ~2%) auto-LPDI, MHAI is virtually excluded (see Figure 2). Catheter angiography can be obviated in these patients. In patients with auto-LPDI greater than ~2%, if there is CE on the admission CT, then MHAI is presumed and catheter angiography should be performed. If CE is absent, then catheter angiography should be undertaken only if the auto-LPDI is ≥ 12%. Decision rule 2, which incorporates CEvol, is similar but classifies as negative both patients with a) diminutive foci of hemorrhage < 0.05 mL and b) those with no CE on CT examination. Any patients with foci of CE above this low volume threshold will likely yield MHAI on catheter angiography.

Those with diminutive to no CE may still benefit from catheter angiography if the same ≥12% auto-LPDI threshold is reached.

The positive predictive value was fairly high for binary CE assessment and both decision rules (84.6–87.2). The benefit of the decision rules was primarily related to improved sensitivity and NPV and substantial (32–63%) reduction in false negative exams.

We conclude that precise personalized decision support using quantitative imaging can improve diagnostic accuracy, and potentially reduce missed injury or delays to intervention in patients with no CE on admission CT. The potential for MHAI despite absence of CE on CT scan is a well-known phenomenon but to our knowledge no objective means of assessing arterial bleeding risk based on the extent of liver parenchymal disruption have been heretofore introduced. Our deep learning-based automated method of calculating LPDI was precise and clinically useful for decreasing false negative CT exams in patients without CE. We are currently not aware of deep learning algorithms for automated volumetric segmentation of liver CE. This is a daunting task since CE can extend beyond the confines of the injured organ. Developing and training convolutional neural networks to correctly identify the source of CE on CT of the upper abdomen is non-trivial with no known predicate.

In the meantime, both decision rules suggest that if CE is either absent or miniscule in patients with BHI, if more than ~$1/10^{th}$ of the total liver volume is disrupted, then MHAI is still possible, and if less than ~ $1/10^{th}$ of the total liver volume is disrupted, then in the absence of surgically important injuries to other organs, NOM is likely to be successful without need for angio-intervention.

The liver-specific quantitative imaging information assessed in this study is not meant to be interpreted in a vacuum given the importance of associated injuries and the patient's hemodynamic state (9, 31). Our decision rules may be helpful, particularly in decreasing false negative CT exams and delays to intervention in BHI patients for whom angiography is being considered despite absence of CE on CT exam.

Robust automated deep learning-based quantitative CT visualization and measurement algorithms have been previously reported for non-traumatic liver lesions as well as ill-defined, irregular, and multicompartmental extraperitoneal pelvic hematoma and foci of pelvic CE (15, 32, 33). As computer vision methods and graphics processing hardware continue to evolve, more features of traumatic organ and vascular injury will be quantifiable with explainable results that can be intuitively displayed as contours or partially transparent mask overlays on the source CT images with no burden to diagnostic radiologist, interventionalist, or surgical end-users. Processing through the algorithm pipelines could be performed while the patient is still on the CT table. This constitutes "free" personalized point-of-care image-based precision diagnostics that can be expected to improve decision support and outcome prediction (32).

Limitations of our study are as follows. The study collection period preceded the proposed 2018 AAST modifications for solid organ grading which include binary assessment of CE. It should be noted that the proposed 2018 AAST solid organ injury scales were published as a

brief current opinion paper and the hepatic organ injury scale has not been clinically validated at the time of writing (34). We did not consider volume of hemoperitoneum as a predictor in the present study (35). Additionally, the method does not stratify risk differently by hilar or peripheral location. Accurate segmentation of hemoperitoneum is performed during the portal venous phase since peak organ enhancement during this phase brings hemoperitoneum into relief. The CT protocol during the collection period included portal venous phase imaging through the upper abdomen only, but hemoperitoneum can pool more caudally in the intraperitoneal pelvis and lower paracolic gutters (36). The scanning protocol at University of Maryland/R. Adams Cowley Shock Trauma Center has recently been changed to include two-phase imaging through the abdomen and pelvis, and we are currently investigating the utility of automated quantitative visualization of hemoperitoneum.

Our auto-LPDI method requires further validation using a larger corpus of external multi-institutional data and containerization as deployable software. The study was limited by its retrospective design. Further validation of the clinical decision rules would require prospective inclusion of consecutive patients with BHI on admission CT regardless of intervention or outcome.

Finally, we did not consider venous hepatic bleeding as an outcome. This is typically treated using modalities such as packing, hepatic debridement or resections, electrocautery, and argon beam coagulation (3, 9). We also did not explore the phenomenon of late hemorrhage or rebleeding, which would require assessment of post-operative CT exams (4, 7, 9).

Conclusion

Auto-LPDI was found to be a significant independent predictor of MHAI in patients with blunt hepatic injury that underwent CT prior to angiography. Incorporation of auto-LPDI in decision rules improved diagnostic performance. Classification and regression tree analysis revealed that auto-LPDI thresholds of ≥ 12% and < 1.7% were optimal for ruling in and excluding MHAI respectively in patients with either no CE, or miniscule (<0.05 mL) foci of CE. Auto-LPDI measurements have the potential to improve triage to catheter angiography in BHI patients sufficiently stable to undergo admission trauma CT, particularly in those for whom the absence of CE foci is not dispositive. The deep learning method once containerized as a software application and prospectively validated in a multicenter cohort, could provide precision diagnostic imaging data at the point of care for objective forecasting and decision support with no burden to radiologists and other members of the traumatology team. In the meantime, our data suggest that MHAI is most likely in patients with traumatic disruption of $1/10^{th}$ or more of the total liver volume on visual inspection.

Acknowledgments

Source of funding:

1. NIBIB NIH K08 EB027141-01A1 (PI: David Dreizin, MD)

2. Accelerated Translational Incubator Pilot (ATIP) award, University of Maryland (PI: David Dreizin, MD)

3. RSNA medical student research grant (Tina Chen)

References

1. Matthes G, Stengel D, Seifert J, Rademacher G, Mutze S, Ekkernkamp A. Blunt liver injuries in polytrauma: results from a cohort study with the regular use of whole-body helical computed tomography. World journal of surgery. 2003;27(10):1124–30. [PubMed: 12917767]
2. Dreizin D, Munera F. Blunt polytrauma: evaluation with 64-section whole-body CT angiography. Radiographics. 2012;32(3):609–31. [PubMed: 22582350]
3. Kozar RA, Feliciano DV, Moore EE, Moore FA, Cocanour CS, West MA, Davis JW, McIntyre RC Jr. Western Trauma Association/critical decisions in trauma: operative management of adult blunt hepatic trauma. Journal of Trauma and Acute Care Surgery. 2011;71(1):1–5.
4. Kutcher ME, Weis JJ, Siada SS, Kaups KL, Kozar RA, Wawrose RA, Summers JI, Eriksson EA, Leon SM, Carrick MM. The role of computed tomographic scan in ongoing triage of operative hepatic trauma: A Western Trauma Association multicenter retrospective study. Journal of Trauma and Acute Care Surgery. 2015;79(6):951–6.
5. Letoublon C, Morra I, Chen Y, Monnin V, Voirin D, Arvieux C. Hepatic arterial embolization in the management of blunt hepatic trauma: indications and complications. Journal of Trauma and Acute Care Surgery. 2011;70(5):1032–7.
6. Fang J-F, Chen R-J, Wong Y-C, Lin B-C, Hsu Y-B, Kao J-L, Chen M-F. Classification and treatment of pooling of contrast material on computed tomographic scan of blunt hepatic trauma. Journal of Trauma and Acute Care Surgery. 2000;49(6):1083–8.
7. Coccolini F, Catena F, Moore EE, Ivatury R, Biffl W, Peitzman A, Coimbra R, Rizoli S, Kluger Y, Abu-Zidan FM. WSES classification and guidelines for liver trauma. World Journal of Emergency Surgery. 2016;11(1):50. [PubMed: 27766112]
8. Moore EE, Cogbill TH, Jurkovich GJ, Shackford SR, Malangoni MA, Champion HR. Organ injury scaling: spleen and liver (1994 revision). Journal of Trauma and Acute Care Surgery. 1995;38(3):323–4.
9. Coccolini F, Montori G, Catena F, Di Saverio S, Biffl W, Moore EE, Peitzman AB, Rizoli S, Tugnoli G, Sartelli M. Liver trauma: WSES position paper. World Journal of Emergency Surgery. 2015;10(1):39. [PubMed: 26309445]
10. Mohr AM, Lavery RF, Barone A, Bahramipour P, Magnotti LJ, Osband AJ, Sifri Z, Livingston DH. Angiographic embolization for liver injuries: low mortality, high morbidity. Journal of Trauma and Acute Care Surgery. 2003;55(6):1077–82.
11. Bala M, Gazalla SA, Faroja M, Bloom AI, Zamir G, Rivkind AI, Almogy G. Complications of high grade liver injuries: management and outcomewith focus on bile leaks. Scandinavian journal of trauma, resuscitation and emergency medicine. 2012;20(1):20.
12. Dabbs DN, Stein DM, Scalea TM. Major hepatic necrosis: a common complication after angioembolization for treatment of high-grade liver injuries. Journal of Trauma and Acute Care Surgery. 2009;66(3):621–9.
13. Patil S, Udupi V. Preprocessing to be considered for MR and CT images containing tumors. IOSR journal of electrical and electronics engineering. 2012;1(4):54–7.
14. Zhou Y, Li Z, Bai S, Wang C, Chen X, Han M, Fishman E, Yuille AL, editors. Prior-aware neural network for partially-supervised multi-organ segmentation. Proceedings of the IEEE International Conference on Computer Vision; 2019.
15. Zhou Y, Dreizin D, Li Y, Zhang Z, Wang Y, Yuille A, editors. Multi-Scale Attentional Network for multi-focal segmentation of active bleed after pelvic fractures. International Workshop on Machine Learning in Medical Imaging; 2019: Springer.
16. Dreizin D, Zhou Y, Fu S, Wang Y, Li G, Champ K, Siegel E, Wang Z, Chen T, Yuille AL. A Multiscale Deep Learning Method for Quantitative Visualization of Traumatic Hemoperitoneum at CT: Assessment of Feasibility and Comparison with Subjective Categorical Estimation. Radiology: Artificial Intelligence. 2020;2(6):e190220. [PubMed: 33330848]
17. Chen L-C, Papandreou G, Kokkinos I, Murphy K, Yuille AL. Deeplab: Semantic image segmentation with deep convolutional nets, atrous convolution, and fully connected crfs. IEEE

transactions on pattern analysis and machine intelligence. 2017;40(4):834–48. [PubMed: 28463186]

18. Zhou Y, Dreizin D, Li Y, Zhang Z, Wang Y, Yuille A. Multi-Scale Attentional Network for Multi-Focal Segmentation of Active Bleed after Pelvic Fractures. arXiv preprint arXiv:190609540. 2019.
19. Chartrand G, Cheng PM, Vorontsov E, Drozdzal M, Turcotte S, Pal CJ, Kadoury S, Tang A. Deep learning: a primer for radiologists. Radiographics. 2017;37(7):2113–31. [PubMed: 29131760]
20. Zou KH, Tuncali K, Silverman SG. Correlation and simple linear regression. Radiology. 2003;227(3):617–28. [PubMed: 12773666]
21. Cicchetti DV. Guidelines, criteria, and rules of thumb for evaluating normed and standardized assessment instruments in psychology. Psychological assessment. 1994;6(4):284.
22. Breiman L, Friedman J, Olshen R, Stone C. Classification and regression trees. Wadsworth & Brooks. Cole Statistics/Probability Series. 1984.
23. DeLong ER, DeLong DM, Clarke-Pearson DL. Comparing the areas under two or more correlated receiver operating characteristic curves: a nonparametric approach. Biometrics. 1988:837–45. [PubMed: 3203132]
24. Zou KH, Warfield SK, Bharatha A, Tempany CM, Kaus MR, Haker SJ, Wells WM III, Jolesz FA, Kikinis R. Statistical validation of image segmentation quality based on a spatial overlap index1: scientific reports. Academic radiology. 2004;11(2):178–89. [PubMed: 14974593]
25. Costantini TW, Coimbra R, Holcomb JB, Podbielski JM, Catalano R, Blackburn A, Scalea TM, Stein DM, Williams L, Conflitti J. Current management of hemorrhage from severe pelvic fractures: results of an American Association for the Surgery of Trauma multi-institutional trial. Journal of Trauma and Acute Care Surgery. 2016;80(5):717–25.
26. Dreizin D, Bodanapally UK, Munera F. MDCT of complications and common postoperative findings following penetrating torso trauma. Emergency radiology. 2015;22(5):553–63. [PubMed: 26013026]
27. Becker CD, Gal I, Baer HU, Vock P. Blunt hepatic trauma in adults: correlation of CT injury grading with outcome. Radiology. 1996;201(1):215–20. [PubMed: 8816546]
28. Dreizin D, Bodanapally U, Boscak A, Tirada N, Issa G, Nascone JW, Bivona L, Mascarenhas D, O'Toole RV, Nixon E. CT prediction model for major arterial injury after blunt pelvic ring disruption. Radiology. 2018;287(3):1061–9. [PubMed: 29558295]
29. Dreizin D, Bodanapally UK, Neerchal N, Tirada N, Patlas M, Herskovits E. Volumetric analysis of pelvic hematomas after blunt trauma using semi-automated seeded region growing segmentation: a method validation study. Abdominal Radiology. 2016;41(11):2203–8. [PubMed: 27349420]
30. Miller PR, Croce MA, Bee TK, Qaisi WG, Smith CP, Collins GL, Fabian TC. ARDS after pulmonary contusion: accurate measurement of contusion volume identifies high-risk patients. Journal of Trauma and Acute Care Surgery. 2001;51(2):223–30.
31. Yoon W, Jeong YY, Kim JK, Seo JJ, Lim HS, Shin SS, Kim JC, Jeong SW, Park JG, Kang HK. CT in blunt liver trauma. Radiographics. 2005;25(1):87–104. [PubMed: 15653589]
32. Dreizin D, Zhou Y, Zhang Y, Tirada N, Yuille AL. Performance of a Deep Learning Algorithm for Automated Segmentation and Quantification of Traumatic Pelvic Hematomas on CT. Journal of digital imaging. 2019:1–9. [PubMed: 30030764]
33. Christ PF, Elshaer MEA, Ettlinger F, Tatavarty S, Bickel M, Bilic P, Rempfler M, Armbruster M, Hofmann F, D'Anastasi M, editors. Automatic liver and lesion segmentation in CT using cascaded fully convolutional neural networks and 3D conditional random fields. International Conference on Medical Image Computing and Computer-Assisted Intervention; 2016: Springer.
34. Kozar RA, Crandall M, Shanmuganathan K, Zarzaur BL, Coburn M, Cribari C, Kaups K, Schuster K, Tominaga GT, Committee tAPA. Organ injury scaling 2018 update: Spleen, liver, and kidney. Journal of Trauma and Acute Care Surgery. 2018;85(6):1119–22.
35. Fang J-F, Wong Y-C, Lin B-C, Hsu Y-P, Chen M-F. The CT risk factors for the need of operative treatment in initially hemodynamically stable patients after blunt hepatic trauma. Journal of Trauma and Acute Care Surgery. 2006;61(3):547–54.
36. Battey TW, Dreizin D, Bodanapally UK, Wnorowski A, Issa G, Iacco A, Chiu W. A comparison of segmented abdominopelvic fluid volumes with conventional CT signs of abdominal compartment syndrome in a trauma population. Abdominal Radiology. 2019:1–8. [PubMed: 29967984]

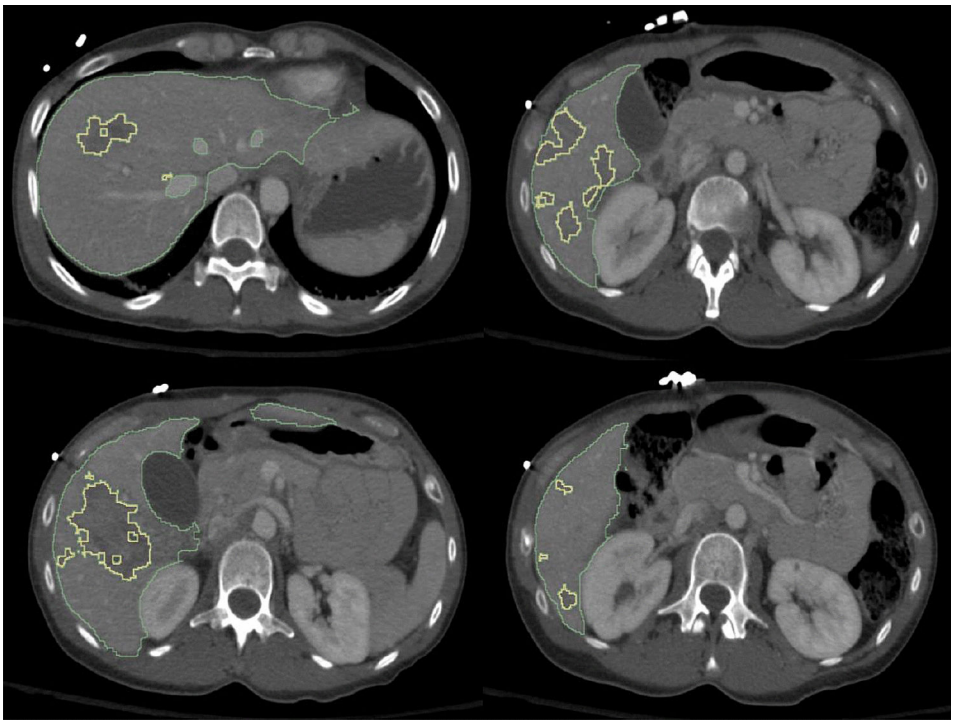

Figure 1.

Figure demonstrates high fidelity of deep learning-based segmentation of both the liver (green contour) and fine irregular margins of multifocal hepatic lacerations with variable shapes and sizes (yellow contour). The LPDI is automatically calculated as % liver disruption over total liver volume and was 13.1% in this example. (LPDI- liver parenchymal disruption index)

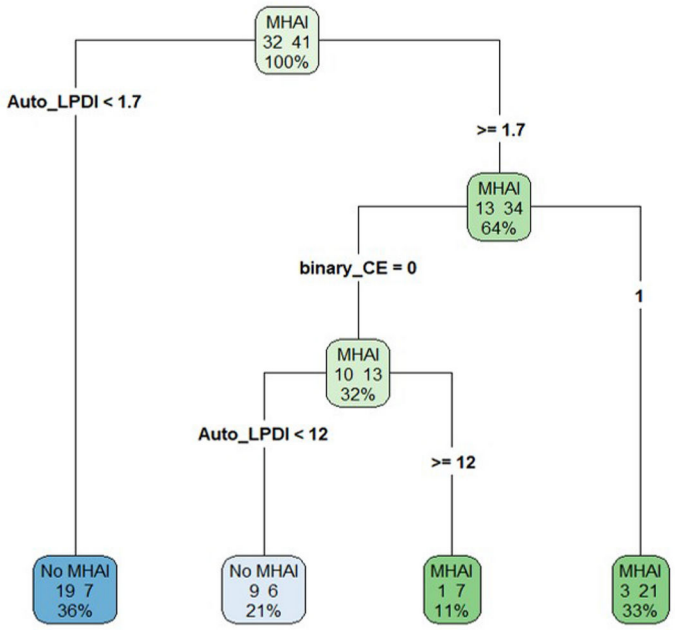

Decision tree 1-Auto-LPD1 and binary CE

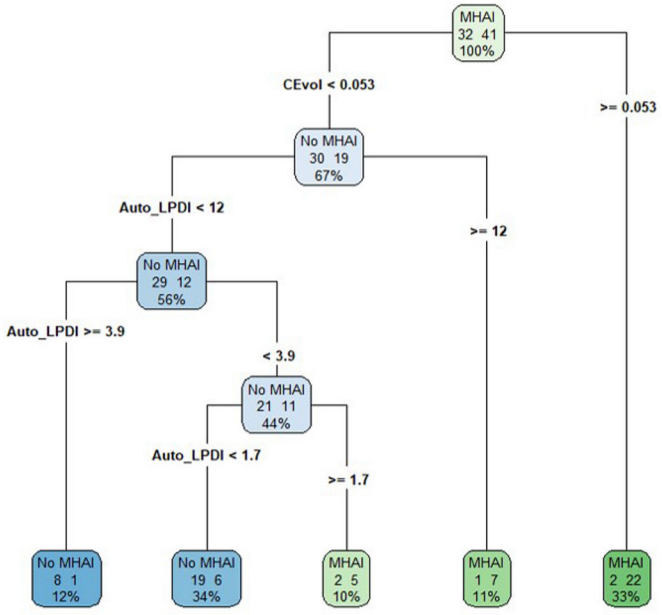

Decision tree 2-Auto-LPD1 and CEvol

Figure 2.

Decision trees from CART analysis are shown. Decision tree 1 includes the combination of auto-LPDI and assessment of CE as a binary sign. Decision tree 2 includes auto-LPDI and CEvol. Contingency table results and AUCs for the two analyses is presented in Table 3. Decision tree analysis revealed an optimal cut off of ≥ 12% for ruling in MHAI when CE is either absent (decision tree 1), or diminutive at < 0.05 mL (decision tree 2). (CART-

classification and regression trees, auto-LPDI- automated liver parenchymal disruption index, CE- contrast extravasation, CEvol- contrast extravasation volume)

Table 1:

Baseline demographic and clinical characteristics

Covariate	Total cohort (n=73)	Institution A* (n=56)	Institution B* (n=17)	Major hepatic arterial injury		P value
				Yes (n= 41)	No (n=32)	
Angio only -n (%)	59 (81)	51 (91)	8 (47)	32 (78)	27 (84)	
Angio and Ex-lap -n (%)	14 (19)	5 (9)	9 (53)	9 (22)	5 (16)	
Age	33 [24 – 52]	29 [23 – 48]	47 [32 – 57]	35 [25 – 53]	32 [23 – 51]	0.734
Gender -n (%)						
Male	40 (55)	30 (54)	10 (59)	25 (61)	15 (47)	0.233
Female	33 (45)	26 (46)	7 (41)	16 (39)	17 (53)	
Mechanism of injury -n (%)						
MVC	56 (77)	41 (73)	15 (88)			
Fall	5 (7)	3 (5)	2 (12)			
Other	12 (16)	12 (21)	0 (0)			
ISS 90	34 [27 – 41]	36 [29 – 42]	34 [25 – 41]	34 [25 – 41]	34 [31 – 44]	0.397
ISS 90 ≥ 16 -n (%)	59 (81)	43 (77)	16 (94)	34 (83)	25 (78)	0.608
Associated injuries -n (%)						
Gallbladder	6 (8)	5 (9)	1 (6)			
Spleen	31 (43)	25 (45)	6 (35)			
Kidney	16 (22)	11 (20)	5 (29)			
Adrenal	18 (25)	13 (23)	5 (29)			
Pancreas	6 (8)	4 (7)	2 (12)			
Colon	3 (4)	3 (5)	0 (0)			
Small Bowel	5 (7)	4 (7)	1 (6)			
Pelvic fracture	17 (23)	13 (23)	4 (24)			
Admission to CT time (min)	50 [31 – 70]	45 [30 – 70]	56 [41 – 67]	50 [31 – 71]	48 [31 – 67]	0.921
Admission to angio time (hours)	4.2 [3.0 – 5.4]	4.4 [3.4 – 5.4]	3.0 [2.6 – 5.4]	3.9 [2.8 – 5.3]	4.4 [3.2 – 6.2]	0.217
Systolic BP (mm Hg)	122 [105 – 133]	121 [105 – 130]	128 [103 – 142]	125 [109 – 133]	120 [101 – 133]	0.267
Hypotension (SBP ≤ 90 mm Hg) -n (%)	7 (10)	4 (7)	3 (18)	3 (7)	4 (13)	0.424
Heart rate	101 [82 – 117]	104 [82 – 116]	95 [86 – 120]	100 [82 – 117]	101 [86 – 113]	0.910
Tachycardia (HR ≥ 90) -n (%)	43 (59)	32 (57)	11 (65)	24 (59)	19 (59)	0.778
In hospital mortality	4§	2	2			

Note.— All continuous variables had non-normal distributions and are presented as median [first quartile - third quartile]

*University of Maryland Medical Center/R. Adams Cowley Shock Trauma Center is denoted as Institution A, and University of Miami Jackson Memorial Medical Center/Ryder Trauma Center is denoted as Institution B.

[§]Three patients expired from unsurvivable head injuries (AIS = 6). One patient expired from multi-organ system failure.

Missing values: there were 3 missing values for systolic blood pressure (4.1%), and three for heart rate (4.1%).

Abbreviations: Angio- angioembolization, ex-lap- exploratory laparotomy, ISS– injury severity score, BP- blood pressure

Table 2:

comparison of results between cohorts

Characteristic	Total cohort	Major hepatic arterial injury		P
		Yes	No	
Auto-LPDI				
n (%)	73	41	32	< **0.001**
mean ± SD	7.73 ± 8.84	11.01 ± 9.98	3.53 ± 4.51	
median [Q1 – Q3]	4.01 [1.00 – 12.05]	10.47 [2.62 – 17.36]	1.36 [0.59 – 5.11]	
range (min, max)	0– 37.79	0.07 – 37.79	0 – 17.58	
CE vol (mL)				
n (%)	73	41	32	< **0.001**
Mean ± SD	1.01 ± 3.16	1.78 ± 4.07	0.03 ± 0.10	
median [Q1 – Q3]	0 [0 – 0.37]	0.07 [0 – 2.00]	0 [0 – 0]	
range (min, max)	0 – 21.4	0 – 21.4	0 – 0.43	
Subcapsular hematoma vol (mL) – n (%) *				
0	70 (96)	38 (93)	32 (100)	0.12
9.70	1 (1)	1 (2)	0 (0)	
49.7	1 (1)	1 (2)	0 (0)	
290.5	1 (1)	1 (2)	0 (0)	
Total	73	41	32	
Hepatic AAST grade – n (%)				
1	0 (0)	0 (0)	0 (0)	0.080
2	6 (8)	1 (2)	5 (16)	
3	24 (33)	13 (32)	11 (35)	
4	39 (53)	25 (34)	14 (45)	
5	3 (4)	2 (5)	1 (3)	
Total	72 **	41	31 **	
CE (binary) – n (%)				
Present	26 (36)	22 (54)	4 (13)	< **0.001**
Absent	47 (64)	19 (46)	28 (87)	

Note.— values are mean +/− SD

Significant p-values are in bold

* only three patients had measurable subcapsular hematoma. Patients are discretized by volumes (0, 9.7, 49.7, 290.5 mL) and presented as number (%)

** One case was not assigned a hepatic AAST grade

Abbreviations: AE- angioembolization, LPDI- liver parenchymal disruption index, CE- contrast extravasation, AAST - American Association for the Surgery of Trauma

Table 3.

Diagnostic performance

Parameter	cut-off value‡	TP	TN	FP	FN	Accuracy	Sensitivity (%)	Specificity (%)	PPV (%)	NPV (%)
Binary CE		22	28	4	19	0.68 (0.57–0.79)	53.7 (37.4–69.3)	87.5 (71.0–96.5)	84.6 (67.8–93.5)	59.6 (50.8–67.7)
Decision tree 1 (LPDI & CEbin)		28	28	4	13	0.77 (0.65–0.86)	68.3 (51.9–81.9)	87.5 (71.0–96.5)	87.5 (71.0–96.5)	68.3 (51.9–81.9)
Decision tree 2 (LPDI & CEvol)		34	27	5	7	0.84 (0.73–0.91)	82.9 (67.9–92.8)	84.4 (67.2–94.7)	87.2 (72.6–95.7)	79.4 (62.1–91.3)
Hepatic AAST ±	2 (1 vs. 2–5)	41	0	31	0	0.57 (0.45–0.69)	100 (91.4–100.0)	0 (0 –11.2)	56.9 (56.9–56.9)	-††
	3 (1–2 vs. 3–5)	40	5	26	1	0.63 (0.50–0.74)	97.6 (87.1–99.9)	16.1 (5.5–33.7)	60.6 (56.7–64.4)	83.3 (38.1–97.6)
	4 (1–3 vs. 4–5)	27	16	15	14	0.60 (0.47–0.71)	65.9 (49.4–79.9)	51.6 (33.1–69.8)	64.3 (54.1–73.4)	43.5 (41.2–45.8)
	5 (1–4, vs. 5)	2	30	1	39	0.44 (0.33–0.57)	4.9 (0.6–16.5)	96.8 (83.3–99.9)	66.7 (16.0–95.5)	43.5 (41.2–45.8)

Note.—

± For hepatic AAST organ injury scale, accuracy metrics are shown for each categorical grade (n =72). One subject was excluded due to missing Hepatic AAST grade

†† NPV not defined because no data is classified as test negative at the specified threshold.

‡ value ≥ cut-off value is defined as test positive

Abbreviations: PPV- positive predictive value, NPV, negative predictive value, LPDI- liver parenchymal disruption index, CE- contrast extravasation, CEbin- contrast extravasation binary, CEvol- contrast extravasation volume, AAST- American Association for the Surgery of Trauma